



A Study on the Production of High-Quality Carbamazepine-Saccharin Co-Crystals: The Role of Seeding Conditions

Khairool A. Mohammad ^{*1}, Kathie L. W. Ping ¹, Nurul A. M. Amin ¹, Engku N. H. E. Zainudin ², Syarifah A. Rahim ¹



CrossMark

¹Faculty of Chemical and Process Engineering Technology, Universiti Malaysia Pahang Al-Sultan Abdullah, 26300 Kuantan, Pahang, Malaysia

²Dept. of Basic Medical Sciences, Kulliyah of Pharmacy, International Islamic University Malaysia (IIUM), 25200 Kuantan, Pahang, Malaysia

Abstract

Seeding involves introducing a pre-formed Carbamazepine-Saccharin (CBZ-SAC) co-crystal into a solution, influenced by seeding temperature, seed size and seed loading. The primary objective of this research is to explore the effects of seeding temperature, seed size and seed loading on the production of CBZ-SAC co-crystals. The seeding experiment was done by adding seed crystal at targeted seeding temperature during the second cooling phase. The experiment was repeated with different seeding temperatures of 20 °C, 25 °C, 30 °C, 35 °C and 40 °C; seed size of <90, 106-125, 125-160 and 160-180 μm; and seed loading of 31.85, 63.70, 95.55 and 127.4 mg. The study reveals that higher seeding temperature and larger crystal size decrease crystal nucleation rate, while higher seed loading increases it. The optimal seeding temperature between 25 °C to 30 °C, with the ideal seed size being 125-160 μm and seed loading is 63.7 mg. In conclusion, the research highlights the critical role of seeding temperature, seed size, and seed loading in the production of CBZ-SAC co-crystals. Additional research focusing on commercialization could involve ADME analysis or solubility test of the co-crystal produced for deeper understanding on the economic advantages associated with CBZ-SAC co-crystal.

Keywords: Seeding; Carbamazepine-Saccharin; Seeding Temperature; Seed Loading; Seed Size; Co-Crystal

1. Introduction

In crystallization, seeding in supersaturated solutions is a crucial process where pre-formed crystals are added to facilitate the formation of the preferred crystalline morphologies in the metastable region. This approach minimizes the need for inclusions, occlusions, and impurities, which are crucial for the generation of quality co-crystals. Seeding is however not simple, it is an intricate phenomenon that locates optimal conditions for effective crystallization by balancing multiple considerations like seed loading, seed size and seeding temperature that play a vital role in controlling both the efficiency and the purity and the yield from the crystallization [1].

Carbamazepine (CBZ), an anti-convulsant agent utilized for the treatment of epilepsy, acute manic episodes, trigeminal neuralgia, and bipolar I disorder [2], is classified as BCS II Class agent having low solubility and high permeability [3]. Enhancing its properties through co-crystallization with saccharin, a co-former, can improve its solubility and bioavailability, potentially reducing side effects [4], [5].

Though promising, there is limited understanding of the aspects governing the crystallization mechanism and the properties of the resulting co-crystals. In this study, we investigate the impact of seeding temperature, seed size and seed loading on the production of Carbamazepine-Saccharin (CBZ-SAC) co-crystals to fill this knowledge gap. The aims are to optimize these parameters and to characterize the newly produced co-crystals in order to improve their solubility and bioavailability.

2. Experimental

2.1 Materials and equipment

Carbamazepine (CBZ) (≥ 99.0 %) and Saccharin (SAC) (≥ 98.0 %) were purchased from Sigma Aldrich. Absolute ethanol (EtOH 99.4%) was used as solvent in co-crystals production. The crystalliser was purchased from Syrris Ltd, which included a 250 mL Syrris Globe® glass-jacketed reactor. Additionally, the reactor was accompanied by the Globe Reactor Master, a system for logging data, and PC software that enabled comprehensive control over the reaction parameters.

*Corresponding author e-mail: kazizul@ump.edu.my (KHAIROOL AZIZUL MOHAMMAD)

Received Date: 01 October 2024, Revised Date: 04 December 2024, Accepted Date: 17 December 2024

DOI: 10.21608/EJCHEM.2024.325215.10560

©2025 National Information and Documentation Center (NIDOC)

2.2 Seed preparation

CBZ and SAC with mole ratio 1:1 which was 3.83 g : 2.97 g were added into 200 ml of ethanol in the vessels. The stirrer was switched on and the temperature of initial suspension was raised to 60°C for a duration of 20 minutes to guarantee the complete dissolution of CBZ and SAC compounds in the ethanol solution. Once the mixture was entirely dissolved, it underwent a gradual cooling process at a rate of 0.8°C/min until crystals were formed, a point determined by turbidity probe. Then, the mixture was reheated for 20 minutes until the turbidity value decreased to below 30%. The mixture was then cooled down at a rate of 0.8°C/min until nucleation was formed in which the turbidity value was increased to 100%. In addition, the crystals were drained and filtered 10 minutes after nucleation was formed. The produced seed crystal was dried in room temperature for 24 hours. Afterward, the seed crystal was collected and sieved using <90 µm, 106-125 µm, 125-160 µm, 160-180 µm, and 180-250 µm of ASTM standard sieve.

2.3 Seeding experiments

CBZ and SAC with mole ratio 1:1 which was 3.83 g : 2.97 g were added into 200 ml of ethanol in the vessels. The stirrer was switched on and the temperature of initial suspension was raised to 60 °C for a duration of 20 minutes to guarantee the complete dissolution of CBZ and SAC compounds in the ethanol solution. After the mixture is completely dissolved, the mixture was cooled down at a cooling rate of 0.8 °C/min until crystals were formed which was determined by turbidity probe. Then, the mixture was reheated until the turbidity value decreased and stabilized, signifying the complete dissolution of crystals. The mixture was then gradually cooled at a rate of 0.8 °C/min until it attained the desired seeding temperature. The seed crystals were added into the solution while adhering to the temperature profile of the solution. The nucleation time and temperature were recorded. The co-crystals were drained and filtered 10 minutes after nucleation was formed. The produced co-crystal was dried in room temperature for 24 hours. Lastly, the produced co-crystals were analysed using Inverted Microscope, Fourier Transform Infrared (FTIR) and Scanning Electron Microscopy (SEM).

2.4 Seed loading

31.85 mg seed crystals of size 125-160 µm were used for seed loading experiment. The targeted seeding temperature was 30 °C. The experiment was repeated with different amounts of seed crystals which were 63.70 mg, 95.55 mg and 127.40 mg.

2.5 Seeding temperature

31.85 mg seed crystals of size 125-160 µm were used for seeding temperature experiment. The targeted seeding temperature was 20 °C. The experiment was repeated with different seeding temperatures which were 25 °C, 30 °C, 35 °C and 40 °C.

2.6 Seed size

31.85 mg seed crystals of size <90 µm were used for seeding temperature experiment. The targeted seeding temperature was 30 °C. The experiment was repeated with different seed sizes which were 106-125 µm, 125-160 µm, and 160-180 µm.

3. Results and discussion

3.1 Analysis on nucleation rate

3.1.1 Effect of seeding temperature

It is demonstrated from Fig. 1 that as seeding temperature increased, the nucleation time of the co-crystal consistently increased which is in line with the principle of crystallization kinetics [6]. Seeding at a temperature of 20 °C resulted in a faster nucleation due to the high supersaturation environment in the solution. Lower temperature often leads to reduced solubility, resulting in a more supersaturated region that is favourable for crystal nucleation and speeds up the nucleation process [7]. In contrast, seeding at 40 °C required a longer nucleation time for co-crystal formation. Elevating the seeding temperature increases crystal component solubility, leading to a less supersaturated solution environment. The system takes an extended period to reach supersaturation levels favourable for effective nucleation causing a delay in crystal formation. Additionally, a clear trend was observed, indicating that an increase in supersaturation correlates with an increase in the nucleation rate. This is in accordance with the finding by Flannigan et al [8].

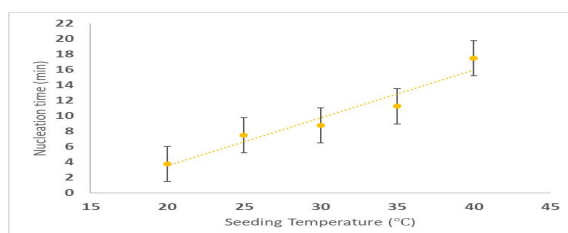


Fig. 1. Effect of seeding temperature on nucleation time

3.1.2 Effect of seed loading

It is showed from Fig. 2 that the graph of the effect of seed loading on the nucleation time in which the nucleation time decreases with seed loading. When 31.85 mg, 63.70 mg, 95.55 mg and 127.40 mg of seed crystals were added at 30 °C, the corresponding average nucleation times were 9.6 min, 7.4 min, 4.4 min and 2.1 min respectively. Higher seed loading accelerates nucleation and potentially reducing processing times. The seed crystals represent the potential nuclei that possess a lower critical free energy when compared to the spontaneous nucleation in the solution. With an increased presence of seeds, additional molecules simply need to adhere to the seed crystal, requiring less energy and thereby facilitating the overall nucleation process. Moreover, the seed provides surface for nucleation to take place. Consequently, higher seed loading results in greater surface area, thereby accelerating the nucleation process [9]. As a result, nucleation occurs more rapidly with a seed loading of 127.4 mg.

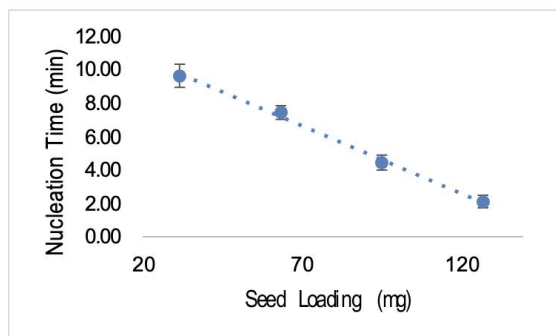


Fig. 2. Effect of seed loading on nucleation time

3.1.3 Effect of seed size

Based on the Fig. 3, the studies depict that the nucleation rate is directly proportional to the seed size. The larger seed size, 160-180 μm resulted in a slower nucleation rate of 7.5 minutes while the smallest seed size produced a higher nucleation rate in 2.5 minutes. According to He et al. [10], the size of the seed significantly influences the nucleation rate for the deposition of the co-crystal molecules onto the surface area of the seed. In general, the larger seed size provides smaller surface area for the growth. The surface area facets provide the interplanar spacing where lattice energy for the interaction between the central molecule, other molecule and the attachment energy [11]. The nucleation dominates over the growth process when the surface areas are small. However, in cases where no surface area available for crystal growth, random crystallization occurs, with nucleation dominating producing and producing crystal nuclei [12].

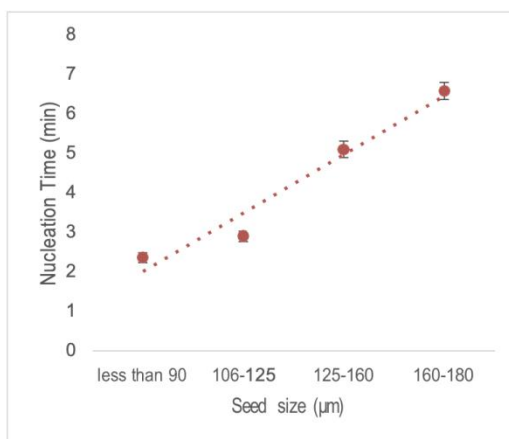


Fig. 3. Effect of seed size on nucleation time

3.2 Analysis on morphology

3.2.1 Effect of seeding temperature

The CBZ-SAC co-crystal's morphology was observed under an inverted microscope, as shown in Fig. 4. Crystals produced at a temperature of 20 °C revealed smaller crystal sizes, as crystal nucleation dominated over crystal growth at higher supersaturation levels. Greater supersaturation levels increased nucleation rate, creating a more restricted growth environment, and resulting in the formation of numerous small crystal nuclei. In contrast, seeding at 40 °C produced greater crystal diameters compared to those synthesized at other temperatures. High temperature seeding led to a higher growth rate and larger crystals due to crystal growth dominating in a low supersaturation environment. This expansion of the seed crystal's

growth window contributed to the production of larger crystal sizes. In general, the size of the crystal increases when the supersaturation level decreases [13], [14].

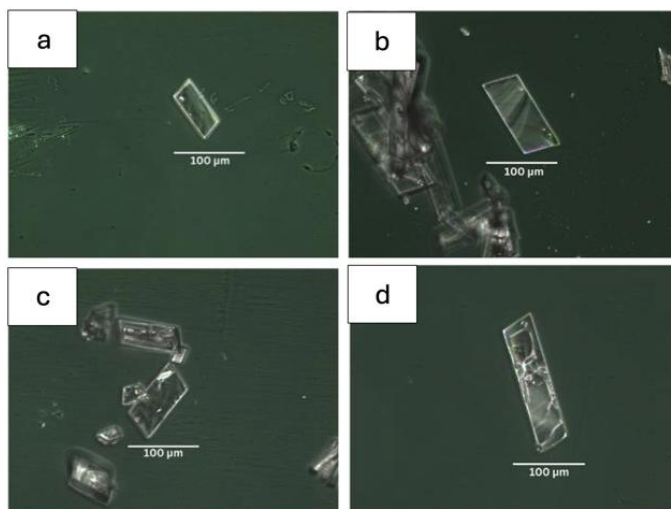


Fig. 4. Inverted microscope images of co-crystal produced with seed loading: (a) 31.85 mg, (b) 63.70 mg, (c) 95.55 mg, (d) 127.4 mg

The SEM results in Fig. 5 showed that the co-crystals produced with seed loading of 31.85 mg, 63.70 mg, 95.55 mg and 127.40 mg have length of 143.0 µm, 149.0 µm, 126.0 µm and 90.2 µm respectively. The size decreases when 95.55 mg and 127.40 mg of seed crystal were added. This can be due to excessive nucleation which had been explained under Inverted Microscopy analysis. The sizes obtained were not similar to the size obtained by using FTIR due to agglomeration of the co-crystals. Agglomeration in co-crystals can arise from attractive forces and process conditions. On the one hand, tiny forces like Van der Waals interactions between co-crystal surfaces can cause loose clinging, known as aggregation [15]. This can be further cemented into more robust agglomerates by solid bridges formed as liquid bridges from solvent evaporation harden. On the other hand, external factors like high agitation in the crystallization vessel increase the frequency of crystal collisions, boosting both aggregation and agglomeration [16], [17].

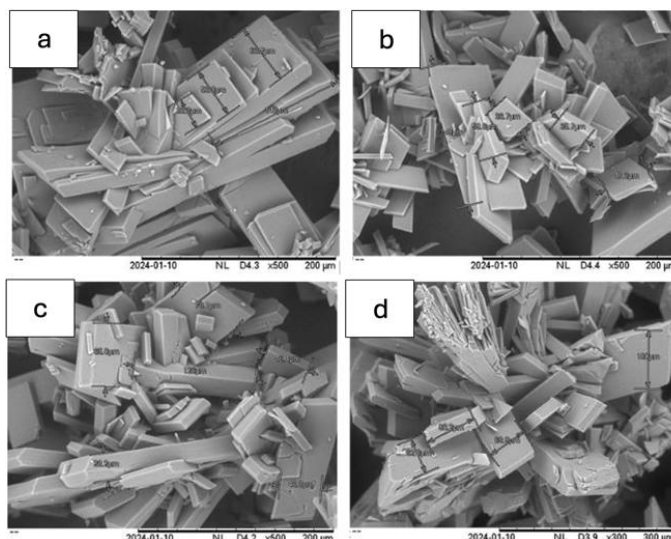


Fig. 5. Scanning Electron Microscope images of co-crystal produced with seed loading: (a) 31.85 mg, (b) 63.70 mg, (c) 95.55 mg, (d) 127.4 mg

3.2.2 Effect of seed size

The microscopic image provided in Fig. 6 shows differences between each of the seed sizes. The less than 90 seed shows small crystal with an average size of a single crystal ≤ 100 µm and some may agglomerate together. The crystal of 106-125

μm produce co-crystal with the size of $\geq 100 \mu\text{m}$. The most significant difference in size of the co-crystals produced is with the seed of 125-160 μm . It produced long and thin crystals with a size of $\geq 200 \mu\text{m}$. The size of the co-crystal produced shows a trend of increment however the 160-180 μm seed shows decrease in crystal size along with the presence of dust particles. Smaller crystals may exhibit a higher nucleation rate and faster growth, resulting in the formation of numerous smaller crystals. Larger crystals, on the other hand, may grow more slowly but achieve a greater size before reaching equilibrium [18]. The larger size can also be found smaller due to the mechanical stress applied to the crystals, such as collisions in the crystallizer's vessel or with the agitator and the attrition between crystals [19].

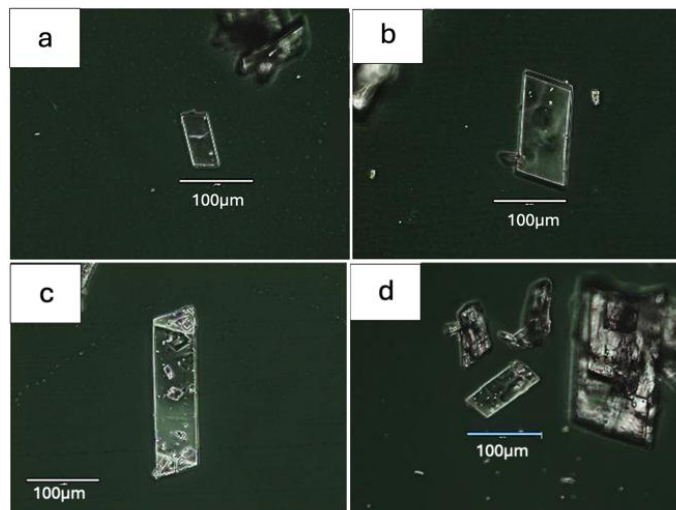


Fig. 6. Inverted microscope images of co-crystal produced by seed size of (a) less than 90 μm (b) 106-125 μm (c) 125-160 μm (d) 160-180 μm .

It is demonstrated in Fig. 7 that, surface morphology of co-crystal produced by 106-125 μm and 160-180 μm . 106-125 μm co-crystal presented rough surface and smooth edges. This may be due to rapid growth of the co-crystallization correlated with the surface area provided. In contrast, 160-180 μm display smooth with surface crystal along with the breakage. The breakage of the crystal causes secondary nucleation which also can act as seed that resulting in dust particles or small particles [20].

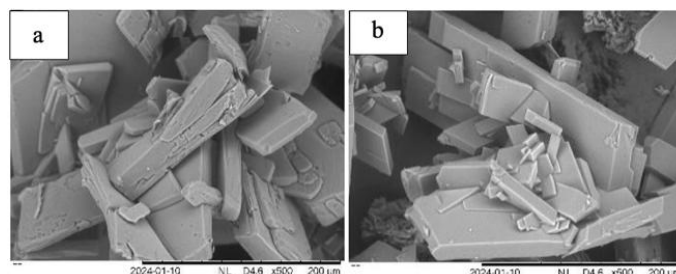


Fig. 7. SEM of co-crystal produced by seed size of (a) 106-125 μm (b) 160-180 μm

3.3 Analysis on functional group present

The FTIR spectrum of carbamazepine as shown in Fig. 8 has double characteristic peaks at 3463.34 and 3154.32 cm^{-1} corresponding to the stretching of amine (N-H), and a characteristic peak at 1603.77 cm^{-1} for the stretching of carbonyl (C=O). The FTIR spectrum of saccharin in Fig. 9 has three characteristic peaks at 3092.25, 1334.65 and 1717.27 cm^{-1} , which indicates the stretching of amine (N-H), sulfonamide (S=O) and carbonyl (C=O) of saccharin. The FTIR spectrum of CBZ-SAC co-crystal displayed in Fig. 10, 11, and 12 under various seeding conditions recorded distinct characteristic peaks compared to the starting material of carbamazepine and saccharin. By comparing to the previous research done by Zhang et al. [1], the shift in the characteristic peaks suggests the occurrence of hydrogen bonding during the co-crystal's formation process.

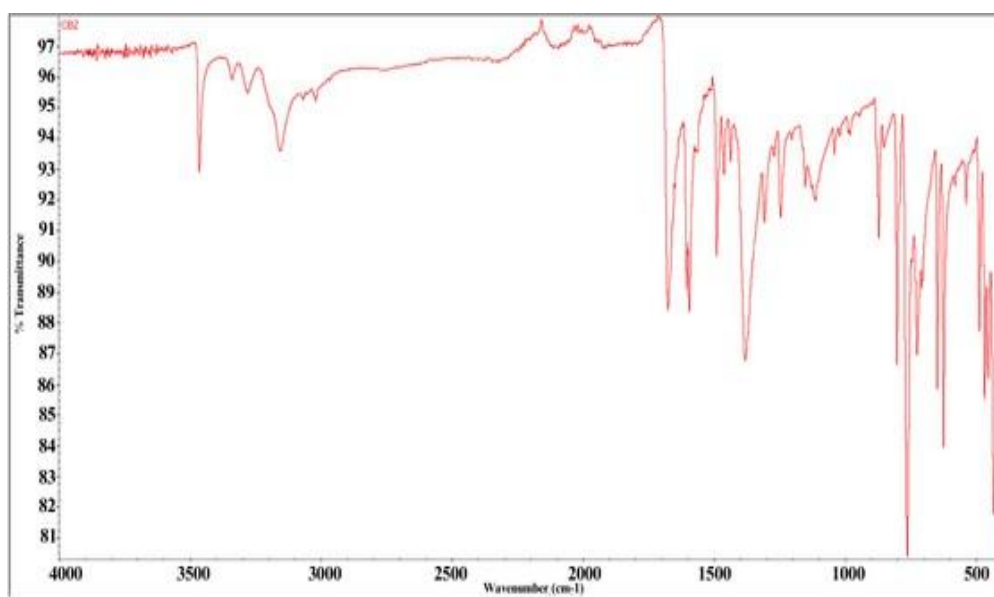


Fig. 8. FTIR spectra of pure carbamazepine

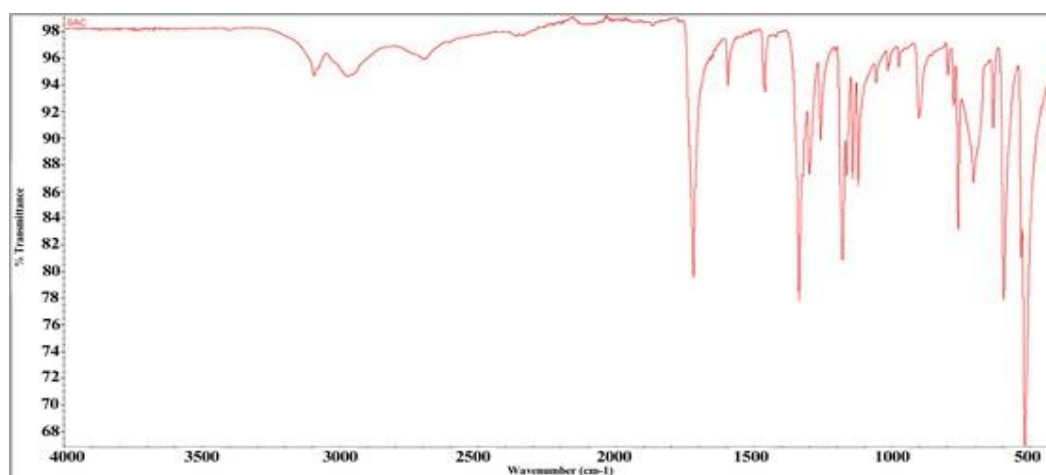


Fig. 9. FTIR spectra of pure saccharin

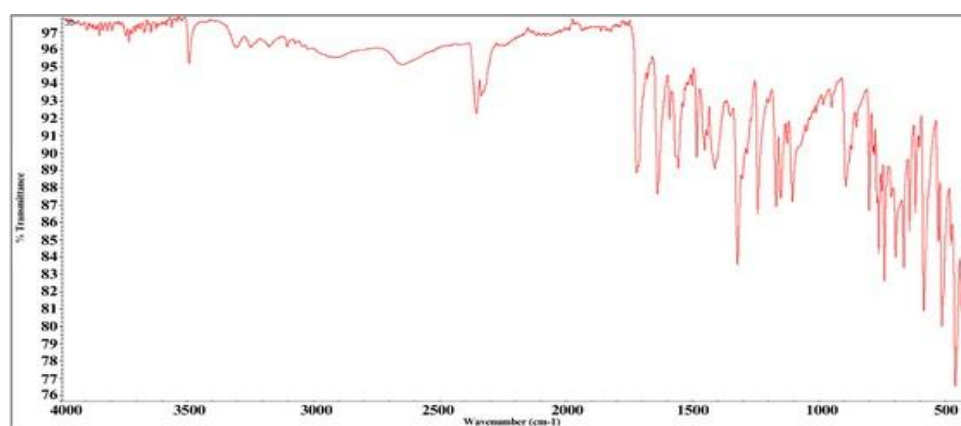


Fig. 10. FTIR spectra of CBZ-SAC co-crystal at seeding temperature 30°C

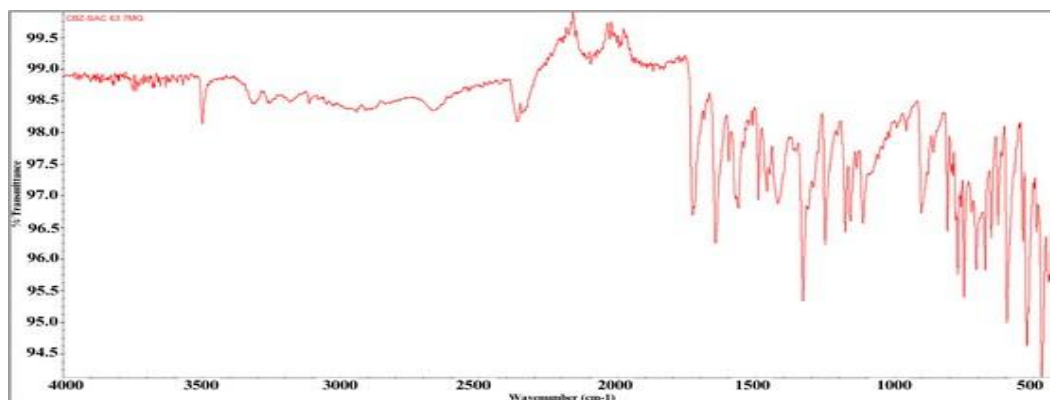


Fig. 11. FTIR spectra of CBZ-SAC co-crystal at seed loading of 63.7mg

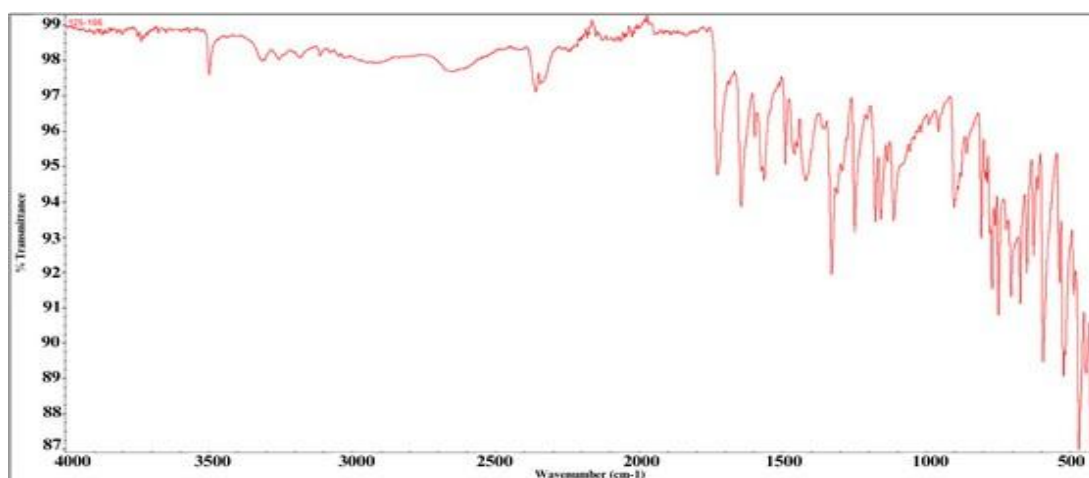


Fig. 12. FTIR spectra of CBZ-SAC co-crystal produced with seed size of 125-160µm

4. Conclusions

The seeding process influences the nucleation rate of crystallization that gives significant impact on the characteristic of the co-crystal. The conducted studies reveal higher seeding temperature and larger crystal sizes leads to slowdown in the crystal nucleation rate. In contrast, higher seed loading amounts increase the nucleation rate. Nevertheless, the morphology through microscopic analysis displayed a plate-like shape of the crystal. FTIR analysis identified and classified the functional group via crystal absorption peak which in carbamazepine are amine and carbonyl group while saccharin shows amine, carbonyl and sulfonamide. Thus, the optimum seeding temperature, seed loading and seed size were determined to be within 25°C to 30°C for seeding temperature, seed size of 125-160µm and seed loading of 63.7mg.

It is ascertained that the studies conducted can be further developed into other studies factors such as different products used with the use of the same or improvise method. For example, the nonsteroidal anti-inflammatory musculoskeletal drug, diclofenac that has the same class as carbamazepine, BCS II Class, may be considered to improve its solubility. Diclofenac tablet is likely to cause stomach ulcer if it is taken for long duration or high dosage. Moreover, the studies also can be refined for the CBZ-SAC co-crystal with the aim of commercializing by conducting research on the ADME analysis or the solubility of the co-crystal produced which can strengthen the objective of acquiring better solubility. Furthermore, this research can be forwarded to the commercial-ready product by considering the patient compliance factors. Patient compliance is the goal of having patient partner in their treatment instead. These can be achieved through the compression of the co-crystal into a convenient form such as tablet.

5. Conflicts of interest

“There are no conflicts to declare”.

6. Formatting of funding sources

The study was supported by the Ministry of Higher Education under UMPA Fundamental Research Grant (RDU230369).

7. Acknowledgments

The authors would like to acknowledge Universiti Malaysia Pahang Al-Sultan Abdullah for the laboratory equipment and facilities.

8. References

- [1] F. Zhang, B. Shan, Y. Wang, Z. Zhu, Z.-Q. Yu, and C. Y. Ma, "Progress and Opportunities for Utilizing Seeding Techniques in Crystallization Processes," *Org Process Res Dev*, vol. 25, no. 7, pp. 1496–1511, 2021, doi: 10.1021/acs.oprd.1c00103.
- [2] J. S. Maan, T. V. H. Duong, and A. Saadabadi, "Carbamazepine," In: StatPearls [Internet]. Treasure Island (FL): StatPearls Publishing. [Online]. Available: <https://www.ncbi.nlm.nih.gov/books/NBK482455/>
- [3] R. Samineni, J. Chimakurthy, and S. Konidala, "Emerging Role of Biopharmaceutical Classification and Biopharmaceutical Drug Disposition System in Dosage form Development: A Systematic Review," *Turk J Pharm Sci*, vol. 19, no. 6, pp. 706–713, 2022, doi: 10.4274/tjps.galenos.2021.73554.
- [4] A. F. Al-Dulaimi, M. Al-kotaji, and F. T. Abachi, "Co-Crystals For Improving Solubility And Bioavailability Of Pharmaceutical Products," *Egypt J Chem*, vol. 65, no. 1, pp. 81–89, 2022, doi: 10.21608/ejchem.2021.77694.3793.
- [5] K. A. Mohammad, M. H. S. Wei, E. N. H. E. Zainudin, and S. Abd Rahim, "Impact of the SAC:CBZ ratio on polymorphic transformation and morphology of carbamazepine-saccharin co-crystals using fast cooling crystallization," *J Therm Anal Calorim*, 2024, doi: 10.1007/s10973-024-13379-y.
- [6] V. Sihorkar and T. Dürig, "The role of polymers and excipients in developing amorphous solid dispersions: An industrial perspective," *Drug Delivery Aspects*, pp. 79–113, 2020, doi: 10.1016/B978-0-12-821222-6.00005-1.
- [7] Y. Zheng, "Size-Independent Nucleation and Growth Model of Potassium Sulfate from Supersaturated Solution Produced by Stirred Crystallization," *Molecules*, vol. 29, no. 1, 2024, doi: 10.3390/molecules29010141.
- [8] J. M. Flannigan, D. MacIver, H. Jolliffe, M. D. Haw, and J. Sefcik, "Nucleation and Growth Kinetics of Sodium Chloride Crystallization from Water and Deuterium Oxide," *Crystals*, vol. 13, p. 1388, 2023, doi: 10.3390/cryst13091388.
- [9] K. A. Mohammad, S. Abd Rahim, and M. R. Abu Bakar, "Kinetics and nucleation mechanism of carbamazepine-saccharin co-crystals in ethanol solution," *Journal of Thermal Analysis and Calorimetry*, vol. 130, no. 3, 2017, doi: 10.1007/s10973-017-6483-1.
- [10] Y. He et al., "Seeding Techniques and Optimization of Solution Crystallization Processes," *Organic Process Research & Development*, vol. 24, no. 10, pp. 1839–1849, 2020, doi: 10.1021/acs.oprd.0c00151.
- [11] P. Klitou, I. Rosbottom, V. Karde, J. Y. Y. Heng, and E. Simone, "Relating Crystal Structure to Surface Properties: A Study on Quercetin Solid Forms," *Crystal Growth and Design*, vol. 22, no. 10, pp. 6103–6113, 2022, doi: 10.1021/acs.cgd.2c00707.
- [12] D. J. Greene, D. Daly, J. J. Doyle, and A. Rafferty, "Caustic-Stable, Controlled-Pore Glass-Ceramics," *Crystal Growth & Design*, vol. 21, no. 2, pp. 809–816, Feb. 2021, doi: 10.1021/acs.cgd.0c01083.
- [13] D. V. Arapov, A. V. Skrypnikov, V. V. Denisenko, I. A. Vysotskaya, and M. A. Zaitseva, "Mathematical Model of Mother Liquor Deposition in Industrial Sugar," *Egyptian Journal of Chemistry*, vol. 65, no. 11, pp. 97–103, Mar. 2022, doi: 10.21608/ejchem.2022.107969.4936.
- [14] G. L. Quilló, S. Bhonsale, B. Gielen, J. F. Van Impe, A. Collas, and C. Xiouras, "Crystal Growth Kinetics of an Industrial Active Pharmaceutical Ingredient: Implications of Different Representations of Supersaturation and Simultaneous Growth Mechanisms," *Crystal Growth & Design*, vol. 21, no. 9, pp. 5403–5420, Sep. 2021, doi: 10.1021/acs.cgd.1c00677.
- [15] P. McArdle and A. Erxleben, "Crystal growth and morphology control of needle-shaped organic crystals," *CrystEngComm*, vol. 26, no. 4, pp. 416–430, 2024, doi: 10.1039/D3CE01041D.
- [16] B. Gielen, J. Jordens, L. C. J. Thomassen, L. Braeken, and T. Van Gerven, "Agglomeration control during ultrasonic crystallization of an active pharmaceutical ingredient," *Crystals (Basel)*, vol. 7, no. 2, Feb. 2017, doi: 10.3390/cryst7020040.
- [17] Y. Xiao, Z. Pan, H. Wang, T. Li, and B. Kong, "Revealing Crystal Aggregates' Evolution through In Situ Visualization in Cooling Crystallization," *Ind Eng Chem Res*, 2024.
- [18] O. Anttila, "Czochralski growth of silicon crystals," in *Handbook of Silicon Based MEMS Materials and Technologies*, Elsevier, 2020, pp. 19–60.
- [19] J. McGinty, N. Yazdanpanah, C. Price, J. H. ter Horst, and J. Sefcik, "Nucleation and Crystal Growth in Continuous Crystallization," in *The Handbook of Continuous Crystallization*, N. Yazdanpanah and Z. K. Nagy, Eds., The Royal Society of Chemistry, 2020, pp. 1–50. doi: 10.1039/9781788013581-00001.
- [20] M. W. Anderson et al., "Understanding crystal nucleation mechanisms: where do we stand? General discussion," *Faraday Discuss*, vol. 235, pp. 219–272, 2022.